Acceptance dependence of fluctuation measures near the QCD critical point

Bo Ling and Mikhail A. Stephanov

Phys. Rev. C **93**, 034915 — Published 28 March 2016

DOI: 10.1103/PhysRevC.93.034915

Acceptance dependence of fluctuation measures near the QCD critical point

Bo Ling and Mikhail A. Stephanov
Physics Department, University of Illinois at Chicago, Chicago, Illinois 60607, USA

We argue that a crucial determinant of the acceptance dependence of fluctuation measures in heavy-ion collisions is the range of correlations in the momentum space, e.g., in rapidity, $\Delta y_{\rm corr}$. The value of $\Delta y_{\rm corr} \sim 1$ for critical thermal fluctuations is determined by the thermal rapidity spread of the particles at freezeout, and has little to do with position space correlations, even near the critical point where the spatial correlation length ξ becomes as large as $2-3$ fm (this is in contrast to the magnitudes of the cumulants, which are sensitive to ξ). When the acceptance window is large, $\Delta y \gg \Delta y_{\rm corr}$, the cumulants of a given particle multiplicity, κ_k, scale linearly with Δy, or mean multiplicity in acceptance, $\langle N\rangle$, and cumulant ratios are acceptance independent. In the opposite regime, $\Delta y \ll \Delta y_{\rm corr}$, the factorial cumulants, $\hat\kappa_k$, scale as $(\Delta y)^k$, or $\langle N\rangle^k$. We demonstrate this general behavior quantitatively in a model for critical point fluctuations, which also shows that the dependence on transverse momentum acceptance is very significant. We conclude that extension of rapidity coverage proposed by STAR should significantly increase the magnitude of the critical point fluctuation signatures.

I. INTRODUCTION

Mapping the QCD phase diagram is one of the most important goals of the heavy-ion collision experiments. A prominent feature on this map of the thermodynamic states of QCD is the critical point punctuating the first order phase transition between hadron matter and quark-gluon plasma phase. Although this scenario is suggested by many models of QCD thermodynamics as well as some lattice calculations, the precise location (in temperature vs baryochemical potential, $T\mu_B$, plane) and even the existence of this point is an open question, which so far has eluded attempts to answer it using theoretical tools, such as first-principle lattice simulations (for reviews, see, e.g., Refs. [1–9]).

The approach pursued by experiments to discover the critical point is based on the analysis of the event-by-event fluctuations [10–12]. In the thermodynamic limit the critical point is a thermodynamic singularity, where the intensive measures of fluctuations violate the central limit theorem and diverge. In a realistic heavy-ion collision this divergence is cut off by the interplay of finite-time, non-equilibrium effects and the effect of the critical slowing down[11, 13, 14]. If, by varying the collision energy $\sqrt{s}$, one can create fireballs with freezeout conditions close to the critical point, one expects to observe non-monotonic dependence of fluctuation measures on $\sqrt{s}$ as the critical point is approached and then passed. The search for the critical point using such beam energy scan strategy is underway at the Relativistic Heavy Ion Collider (RHIC) at the Brookhaven National Laboratory (BNL) and at the Super Proton Synchrotron (SPS) at CERN in Geneva [15–19].

In order to compare experimental measurements with theoretical predictions, as well as the results of different experiments to each other, it is essential to understand the dependence of the fluctuation measures on the size of the detector acceptance window, which varies among experiments, or even different analyses of the same experiment. The goal of the paper is to elucidate and quantify this dependence.

The focus of this work is on critical point signatures. In particular, on the higher-order cumulants sensitive to the thermodynamic conditions at freezeout [20, 21] and especially to the critical fluctuations [22]. However, we begin with a more general analysis of acceptance dependence, which we then illustrate using the critical point fluctuations. The purpose of this paper is to examine the physics behind this dependence and demonstrate it in a simple, analytic, but quantitatively realistic model. Our qualitative arguments and quantitative results complement and extend analyses of the acceptance dependence of the critical fluctuations in Refs.[1, 23] to higher-order cumulants, and also complement and contrast the analyses of Refs.[24–31] of non-critical correlations (see also reviews [12, 32] for further references).

The type of questions we wish to answer are, for example, what is the effect on critical point signatures of increasing the transverse momentum range, say, from $p_T \in (0.4, 0.8)$ GeV to $(0.4, 1.2)$ GeV, as has been done in the recent analysis by STAR [33]? Or, what is the effect of extending the rapidity window from $\Delta y = 1$ to $\Delta y = 1.5$ for protons, which will result from upgrading the inner sectors of the Time Projection Chamber (iTPC) proposed [34] by the STAR experiment at RHIC?

II. ACCEPTANCE DEPENDENCE OF CUMULANTS

Our main goal is to provide a transparent description of the acceptance dependence of fluctuation measures, which can be used to build quantitatively precise tools necessary to extract physics from experimental data. To prevent the complexity of the heavy-ion collision from obscuring the relevant features we wish to highlight, we start with the simplest idealized Bjorken model [35] of a boost invariant fireball and consider the dependence of the fluctuation measures on the rapidity acceptance window Δy. This will allow us to gain understanding of the

main characteristics of the acceptance dependence, which we can then carry over to a more realistic model with transverse expansion and p_T acceptance dependence.

Let us denote the number, or multiplicity, of accepted particles of a given species (e.g., protons or pions) by N.[1] The mean over all events, $\langle N\rangle$, is then proportional to Δy due to the boost invariance:

$$\langle N\rangle \sim \Delta y. \tag{1}$$

How do the cumulants of order k, $\kappa_k[N]$, of N vary with Δy? The answer crucially depends on the range of the correlations in rapidity, which we denote by $\Delta y_{\rm corr}$.

Different contributions to the correlations (initial conditions, HBT, thermal/hydro fluctuations, critical fluctuations, etc.) are characterized by different $\Delta y_{\rm corr}$. In this paper we shall focus on critical point fluctuations, but we begin with a more general discussion of correlations and their effect on acceptance dependence.

It is important to distinguish two qualitatively different regimes: $\Delta y \gg \Delta y_{\rm corr}$ and $\Delta y \ll \Delta y_{\rm corr}$.

When $\Delta y \gg \Delta y_{\rm corr}$, all cumulants grow linearly with Δy, because uncorrelated contributions are additive, by construction, in a cumulant. It is convenient and customary to remove this trivial volume dependence by normalizing cumulants by their trivial, uncorrelated (Poisson) value ($\langle N\rangle$, for cumulants of N), defining

$$\omega_k \equiv \frac{\kappa_k}{\langle N\rangle}. \tag{2}$$

The contribution of physical (e.g., critical) correlations to this quantity, $(\omega_k - 1)$, saturates at a constant value for $\Delta y \gg \Delta y_{\rm corr}$.[2]

In the opposite regime, $\Delta y \ll \Delta y_{\rm corr}$, since the cumulants approach Poisson distribution values in the limit $\Delta y \sim \langle N\rangle \to 0$, we shall focus on the deviation of the cumulants from their Poisson value, $\kappa_k - \langle N\rangle$. It is convenient to express $\kappa_k - \langle N\rangle$ as a linear combination of factorial cumulants, $\hat\kappa_l$, of equal or lower orders

$$\kappa_k - \langle N\rangle = \hat\kappa_k + \sum_{l=2}^{k-1} S(k,l)\hat\kappa_l \tag{3}$$

where $S(n,m)$ are Stirling numbers of the second kind. The most useful property of the factorial cumulants is that each $\hat\kappa_k$ measures the strength of the (connected) k-particle correlation, and is therefore proportional to the number of correlated k-plets, which scales roughly as N^k, i.e., $(\Delta y)^k$. This property is known (see, e.g., Ref.[36] and references therein), but for completeness and to provide a better intuitive understanding we derive it for $k \le 4$ in Appendix A.

Because of the simple asymptotic behavior of the factorial cumulants in both regimes of Δy:

$$\hat\kappa_k \sim \Delta y \sim \langle N\rangle \qquad (\Delta y \gg \Delta y_{\rm corr}) \tag{4}$$

and

$$\hat\kappa_k \sim (\Delta y)^k \sim \langle N\rangle^k \qquad (\Delta y \ll \Delta y_{\rm corr}), \tag{5}$$

it is more convenient to describe acceptance dependence in terms of the factorial cumulants $\hat\kappa_k$.

In contrast, the behavior of the normal cumulants, κ_k, in the regime $\Delta y \ll \Delta y_{\rm corr}$ is more complicated. According to Eqs. (3) and (5), the limit $\Delta y \to 0$ is controlled by the lowest cumulant, $\hat\kappa_2$, i.e.,

$$\kappa_k - \langle N\rangle \sim \hat\kappa_2 \sim (\Delta y)^2 \qquad \text{when } \Delta y \to 0, \tag{6}$$

or $\omega_k - 1 \sim \Delta y$.[3] On the other hand, if or when the approximate hierarchy $|\hat\kappa_k| \gg |\hat\kappa_l|$ for $k > l$ holds, as experimental results [33] indicate at some energies (e.g., at $\sqrt{s} = 7.7$ GeV $|\hat\kappa_4| \gg |\hat\kappa_3|, |\hat\kappa_2|$ for $\Delta y \sim 1$), the scaling in the regime $\Delta y \ll \Delta y_{\rm corr}$, but not too small, could be dominated by the highest cumulant in Eq. (3), and then

$$\kappa_k - \langle N\rangle \sim \hat\kappa_k \sim (\Delta y)^k \qquad (\Delta y \text{ not too small}), \tag{7}$$

or $\omega_k - 1 \sim (\Delta y)^{k-1}$. The crossover between this behavior and that in Eq. (6) could be a source of non-monotonic acceptance dependence of ω_k in some cases.

III. CRITICAL POINT CORRELATIONS

In order to describe the acceptance dependence of the fluctuation measures (the cumulants) more quantitatively we need to input the physical information about the correlations. We shall focus on *critical point* contribution to the fluctuations and use the model described in Ref. [11, 23] and, in application to higher-order cumulants, in Refs. [22, 37, 38]. In this model the multiplicity fluctuations at freezeout near the critical point receive a contribution due to the coupling of the critical mode σ – a collective mode of fluctuations whose correlation length ξ becomes large (and diverges at the critical point in the theoretical limit of infinitely large system size and lifetime).

[1] The acceptance dependence of the fluctuations of a particle number as opposed to, e.g., net-proton or net-charge, is considerably more transparent and allows us to focus on the most important features.

[2] Eq. (2) is not the only natural way to normalize the cumulant. Another widely used normalization is κ_k/κ_2. Since, in practice, $\kappa_2 - \langle N\rangle \ll \langle N\rangle$, there is little difference between this normalization and Eq. (2).

[3] This helps explain the linear dependence of the normalized cumulants as the acceptance $\Delta \to 0$ in Ref.[28]. We thank M. Kitazawa for a discussion of this point.

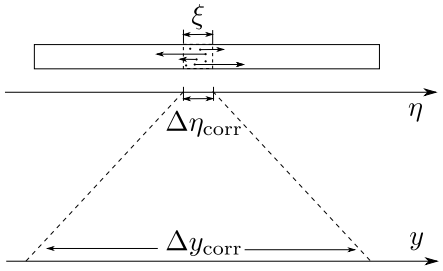

FIG. 1. Schematic illustration of the relation between the spatial (Bjorken) rapidity η and kinematic rapidity y via the effect of the thermal broadening (freezeout smearing).

A. The range of correlations

What determines $\Delta y_{\rm corr}$? This depends on the physics behind the correlations and, in the case we consider, the critical point, it is the fluctuating collective mode. Consider the boost-invariant scenario with the correlation length in co-moving coordinates at freezeout given by ξ (Fig. 1). This translates into Bjorken rapidity correlation length $\Delta\eta_{\rm corr} \approx \xi/\tau_{\rm f}$. With ξ ranging from 1 fm typically to about $2-3$ fm near the critical point [13] and with freezeout Bjorken time $\tau_{\rm f} \sim 10$ fm one estimates $\Delta\eta_{\rm corr} \sim 0.1-0.3$.

Detectors, however, do not measure the position space (Bjorken) rapidity η, but the kinematic rapidity y of the particles. Within the spatial correlation volume $\Delta\eta_{\rm corr}$ at freezeout thermal distribution of particle rapidities y_p in the co-moving frame ranges roughly from -1 to 1 (Fig. 2). The observed rapidity $y = \eta + y_p$ of the particles from each correlated volume is then spread over an interval of order $\Delta y_{\rm corr} \sim 1$ (Fig. 1). Such thermal broadening, or freezeout smearing, in the translation of hydrodynamic spatial correlations into kinematic correlations has been discussed recently in, e.g., Refs.[39, 40]. Because $\Delta y_{\rm corr} \gg \Delta\eta_{\rm corr}$, the value of $\Delta y_{\rm corr}$ is not sensitive to ξ. This is in contrast to the magnitude of $\omega_k - 1$ [22] — larger ξ means more correlated particles in the same $\Delta y_{\rm corr}$ and larger value of $\omega_k - 1$.

It is essential for this argument that, within the correlated spatial volume, particles of all momenta in the thermal distribution are correlated with each other, as they are in the case of the critical point fluctuations we consider — see Eq. (14) below.

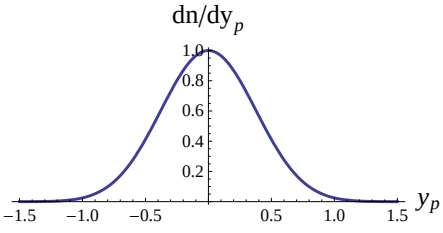

FIG. 2. Thermal proton rapidity distribution ($T = 160$ MeV).

B. The model of critical correlations

To make calculations simpler and the results more transparent, we shall use the observation that even the maximal correlation length $\xi \lesssim 2-3$ fm (limited in a heavy-ion collision by finite-time and critical slowing down effects [13]) is still considerably smaller than the typical size of the system. A measure of that size is either the transverse radius or the Bjorken proper time at freezeout, $R \sim 7-10$ fm. In the idealized limit $R \gg \xi$ we can consider the spatial correlation as almost local and approximate it by a delta function in the integrals involving slowly (in position space) varying distribution functions $f(\boldsymbol{x},\boldsymbol{p})$. The normalization of the delta function is fixed by matching the space integral of the correlator:

$$\int d^3\boldsymbol{x}\langle\sigma(\boldsymbol{x})\sigma(\boldsymbol{y})\rangle = T\xi^2 \;\Rightarrow\; \langle\sigma(\boldsymbol{x})\sigma(\boldsymbol{y})\rangle \to T\xi^2\delta^3(\boldsymbol{x}-\boldsymbol{y}) \tag{8}$$

Similar approach can be applied to the 3-point and 4-point (connected) functions, which can be also approximated by delta-functions, normalized using the results of Ref.[22]:

$$\langle\sigma(\boldsymbol{x})\sigma(\boldsymbol{y})\sigma(\boldsymbol{z})\rangle \to -2\tilde\lambda_3 T^{3/2}\xi^{9/2}\delta^6(\boldsymbol{x},\boldsymbol{y},\boldsymbol{z}), \tag{9}$$

where $\delta^6(\boldsymbol{x},\boldsymbol{y},\boldsymbol{z}) \equiv \delta^3(\boldsymbol{x}-\boldsymbol{y})\delta^3(\boldsymbol{x}-\boldsymbol{z})$ and

$$\langle\sigma(\boldsymbol{x})\sigma(\boldsymbol{y})\sigma(\boldsymbol{z})\sigma(\boldsymbol{w})\rangle_c \to 6(2\tilde\lambda_3^2 - \tilde\lambda_4)T^2\xi^7\delta^9(\boldsymbol{x},\boldsymbol{y},\boldsymbol{z},\boldsymbol{w}), \tag{10}$$

where $\delta^9(\boldsymbol{x},\boldsymbol{y},\boldsymbol{z},\boldsymbol{w}) \equiv \delta^3(\boldsymbol{x}-\boldsymbol{y})\delta^3(\boldsymbol{x}-\boldsymbol{z})\delta^3(\boldsymbol{x}-\boldsymbol{w})$. The parameters $\tilde\lambda_3$ and $\tilde\lambda_4$ are dimensionless functions of T and μ_B characterizing the non-gaussianity of the fluctuations of σ and described in more detail in Ref.[22]. We shall not be concerned with the *absolute* magnitude of (the critical contribution to) the cumulants in this paper. Therefore, the normalization factors, such as $\tilde\lambda_3$ and $\tilde\lambda_4$, will not be essential in the following.

The contribution of the critical mode to the fluctuation of the particle distribution function, f_A, is given by [37]

$$(\delta f_A)_\sigma = -\frac{\chi_A}{\gamma_A} g\sigma(\boldsymbol{x}_A), \tag{11}$$

where we introduced a shorthand for the set of phase-space coordinates, e.g.,

$$f_A \equiv f(\boldsymbol{x}_A,\boldsymbol{p}_A,s_A) \tag{12}$$

with the species index s_A standing for any additional particle quantum numbers (spin, charge, etc.). We denoted the derivative of the equilibrium distribution function, $f_A^{\rm eq} = (\exp(\epsilon_A-\mu)/T) \pm 1)^{-1}$, by

$$\chi_A \equiv \frac{\partial f_A^{\rm eq}}{\partial\mu} = \frac{1}{T} f_A^{\rm eq}(1 \pm f_A^{\rm eq}), \tag{13}$$

(plus/minus for fermions/bosons), where the coupling g is defined as derivative of the effective mass of the particle in a given background of the critical mode:

$g \equiv dm(\sigma)/d\sigma$. For protons this corresponds to effective sigma-model coupling $g\sigma\bar{\Psi}\Psi$. We also denoted by $\gamma_A = d\epsilon_A/dm = m/\epsilon_A$ the relativistic gamma-factor of the particle with momentum $\boldsymbol{p}_A$.

Using Eq. (11) we can calculate correlators of these critical fluctuations. For example, for the critical contribution, denoted by $\langle \ldots \rangle_\sigma$, to the two-point correlator we find

$$\langle \delta f_A \delta f_B \rangle_\sigma = T\xi^2 g^2 \frac{\chi_A}{\gamma_A}\frac{\chi_B}{\gamma_B}\delta^3(\boldsymbol{x}_A - \boldsymbol{x}_B). \tag{14}$$

Note that the correlation in Eq. (14) appears local in the position space (on scales $R \gg \xi$), but it is non-local in the momentum space. This momentum space non-locality is essential for the argument in Section III A.

Introducing the shorthand notation

$$\int_A \equiv \int \frac{d^3\boldsymbol{x}_A\, d^3\boldsymbol{p}_A}{(2\pi)^3} \sum_{s_A} \tag{15}$$

for the integration over the phase space, i.e., over $\boldsymbol{x}_A$, $\boldsymbol{p}_A$ (as well as the summation over spin and other quantum numbers) we can express the fluctuation of the particle number N in terms of δf: $\delta N = \int_A \delta f_A$. The critical contribution to the quadratic cumulant of the fluctuations is then given by

$$\kappa_2[N]_\sigma \equiv \langle (\delta N)^2 \rangle_\sigma = \int_A \int_B T\xi^2 g^2 \frac{\chi_A}{\gamma_A}\frac{\chi_B}{\gamma_B}\delta^3(\boldsymbol{x}_A - \boldsymbol{x}_B) \tag{16}$$

One of the spatial integrals (say, over $\boldsymbol{x}_B$) can be performed using the delta-function. The result can be written as

$$\kappa_2[N]_\sigma \equiv \langle (\delta N)^2 \rangle_\sigma = \int d^3\boldsymbol{x}\; T\xi^2 g^2 \left(\int \frac{d^3\boldsymbol{p}}{(2\pi)^3} \sum_s \frac{\chi}{\gamma} \right)^2 \tag{17}$$

The dependence on the acceptance enters via the range of the momentum integration in Eq. (17). This range is fixed in the frame of the detector (lab frame), but translates (by boost) into different ranges in the co-moving frame for different points on the freezeout surface.

Treating higher-order cumulants similarly we find

$$\kappa_3[N]_\sigma \equiv \langle (\delta N)^3 \rangle_\sigma = \int d^3\boldsymbol{x}\; 2\tilde{\lambda}_3 T^{3/2}\xi^{9/2} g^3 \left(\int \frac{d^3\boldsymbol{p}}{(2\pi)^3} \sum_s \frac{\chi}{\gamma} \right)^3 \tag{18}$$

and

$$\kappa_4[N]_\sigma \equiv \langle (\delta N)^4 \rangle_\sigma - 3\langle (\delta N)^2 \rangle_\sigma^2 = \int d^3\boldsymbol{x}\; 6\left(2\tilde{\lambda}_3^2 - \tilde{\lambda}_3\right) T^2\xi^7 g^4 \left(\int \frac{d^3\boldsymbol{p}}{(2\pi)^3} \sum_s \frac{\chi}{\gamma} \right)^4 \tag{19}$$

Our model of the critical fluctuations is not precise or detailed enough to distinguish between factorial, $\hat{\kappa}_k$, and normal cumulants $\kappa_k - \langle N \rangle$. However, it is clear from the physical origin (k-particle correlation) and from the small Δy behavior of $\kappa_k[N]_\sigma$, that they describe contributions to the factorial cumulants $\hat{\kappa}_k$. However, the model describes the regime of sufficiently large correlation length ξ, when critical contributions are proportional to higher powers of ξ for higher cumulants, $\hat{\kappa}_k \sim \xi^{5k/2-3}$ [22], thus leading to the approximate hierarchy $|\hat{\kappa}_4| \gg |\hat{\kappa}_3| \gg |\hat{\kappa}_2|$.

If such hierarchy does not hold in the data (in particular, when $\hat{\kappa}_4$ is close to zero because it changes sign [37], or when Δy is very small), one should then directly compare $\kappa_k[N]_\sigma$ to experimentally measured factorial cumulants, $\hat{\kappa}_k$, instead of $\kappa_k - \langle N \rangle$.

C. Transverse expansion

We shall use the blast wave model (see, e.g., Refs. [41, 42] and, in application to transverse momentum correlations, Refs. [40, 43–45]) of the freezeout surface to perform the integrals in Eqs. (17)–(19). In this model the freezeout surface is isochronous, at a given Bjorken time $\tau = \tau_{\rm f}$, and the 4-velocity field is given, in longitudinal Bjorken coordinates (τ, η) and transverse polar coordinates (r, ϕ), as

$$(u^\tau, u^\eta, u^r, u^\phi) = (\cosh\eta_\perp, 0, \sinh\eta_\perp, 0), \tag{20}$$

where the transverse velocity is parameterized as

$$\beta_\perp \equiv \tanh\eta_\perp \equiv \frac{u^r}{u^\tau} = \beta_s \frac{r}{R}, \tag{21}$$

where the surface velocity $\beta_s \approx 0.6$ is a parameter we determine by fitting the inclusive single-particle distribution.

The space integral in Eqs. (17)–(19) becomes the integral over the freezeout hypersurface:

$$\int d^3\boldsymbol{x} \to \tau \int d\eta \int r dr \int d\phi. \tag{22}$$

The momentum integration in Eqs. (17)–(19) can be expressed as an integral over kinematic rapidity, transverse momentum $p_\perp$ and azimuthal angle ψ:

$$\int \frac{d^3\boldsymbol{p}}{(2\pi)^3} \sum_s \frac{1}{\gamma} \to \frac{d_{\rm s} m}{(2\pi)^3} \int_{y_1}^{y_2} dy \int_{p_{\rm min}}^{p_{\rm max}} p_\perp dp_\perp \int_0^{2\pi} d\psi, \tag{23}$$

where d_s is the species degeneracy (e.g., $d_{\rm s} = 2$ for proton spin). The acceptance cuts are represented by the limits of the integrations, with $y_2 - y_1 \equiv \Delta y$. The particle distribution function is given in terms of the energy $\epsilon_{\boldsymbol{p}} = u \cdot p$ in the co-moving frame and expressed in terms of the lab frame y, $p_\perp$ and ψ, as well as η, r and ϕ, via

$$u \cdot p = m_\perp \cosh(y - \eta)\cosh\eta_\perp - p_\perp \cos(\psi - \phi)\sinh\eta_\perp, \tag{24}$$

where $m_\perp \equiv \sqrt{m^2+p_\perp^2}$ and $\eta_\perp$ is given by Eq. (21). Boltzmann approximation for the equilibrium distribution function

$$f^{\rm eq} \approx \exp\left(\frac{\mu - u\cdot p}{T}\right), \qquad \chi \approx \frac{f^{\rm eq}}{T}, \tag{25}$$

is sufficient for our purposes (in particular, for protons, assuming $m-\mu_B \gg T$), and it allows performing part of the multiple integration in Eqs. (17)–(19) analytically.

D. Beyond the model

Before proceeding to discuss the results let us emphasize again that one of our simplifying approximations is that of Bjorken (boost) invariance of the freezeout hypersurface. This assumption does not affect the validity of Eqs. (17)–(19). The formulas are more general and can be applied also for a realistic freezeout surface obtained in a hydrodynamic simulation, as it is done in Ref.[46]. The purpose of our paper is to address the issue of the acceptance dependence in a transparent fashion. The use of the Bjorken scenario (with a blast-model transverse flow) allows us to separate the acceptance window size dependence from, e.g., the dependence on the location of the acceptance window (central vs forward rapidity), which has a completely different physical origin.

The approximation $R \gg \xi$, as in, e.g., Eq. (8), is also very helpful to simplify our treatment, but can be relaxed, if necessary, along the lines of Refs.[46, 47]. To be consistent, however, this should be accompanied by the inclusion of finite-time, non-equilibrium effects.

We need to keep in mind that the model we use to demonstrate the acceptance dependence is the most basic model of critical fluctuations, which neglects non-equilibrium effects except for one – the critical slowing down effect limiting the magnitude of ξ. Nevertheless, the model should be sufficient to describe qualitatively and semiquantitatively the acceptance dependence of the cumulants, largely because this dependence is constrained by generic considerations described in Section II.

The most important feature of this dependence is $\Delta y_{\rm corr}$, which is determined by the thermal momentum distribution of the particles at freezeout, and is not much sensitive to the dynamics of the spatial correlations. The feature of the critical fluctuations which is very important for both Δy and p_T window dependence of the fluctuations is the non-locality of the correlations in the *momentum* space, e.g., in Eq. (14). We do not expect that taking into account non-equilibrium effects more thoroughly (along the lines of, e.g., Ref.[47] or [48]) will affect this property significantly.

We do wish, however, to underscore the importance of developing a more comprehensive non-equilibrium approach to fluctuations to enable more quantitative comparison with experiment [49]. Such an approach is especially crucial for predicting the absolute magnitudes of the cumulants (which sensitively depend on ξ [22]) as well as their sign [37, 48, 50].

Finally, we wish to emphasize again that many effects determining the magnitude of the correlations and their acceptance dependence are left beyond the scope of the paper. These are physical effects, such as that of the initial state fluctuations (baryon stopping, jets, etc.), charge or baryon number conservation effects, directed flow, final state rescattering, etc., as well as instrumental effects, such as efficiency dependence on the detector occupancy, particle momenta or the location of the sector boundaries. Many of these questions have been addressed, or will be addressed by other theoretical and experimental work. There is still much to be done.

The goal of the paper is to focus on the physical mechanisms directly related to critical fluctuations. Furthermore, we do not attempt to address the energy dependence, which has been studied elsewhere, but the effect of acceptance at a given collision energy.

We expect our results to be correct on a qualitative and semiquantitative level, in particular, because they satisfy the general considerations in Section II. We hope our paper will serve as a guide for experiments attempting to compare measurements at different acceptance. However, more precise comparison and interpretation of data would require careful analysis of other relevant effects.

IV. RESULTS

We can now use the formulas we derived for critical point contributions to (factorial) cumulants to predict the acceptance dependence of these contributions. We choose $\sqrt{s} = 19.6$ GeV as a representative collision energy. The results are very similar at other energies we considered (e.g., 7.7 and 11.5 GeV) and in agreement with the general arguments described in Section II.

We determine the temperature and chemical potential at freezeout using the fit from Ref. [51]: $T \approx 160$ MeV, $\mu_B \approx 200$ MeV.

We use the value of β_s (the radial surface velocity) optimizing the agreement with the proton p_T spectrum, as shown in Fig. 3.

We normalize the proton cumulants $\kappa_k[N]$ by their Poisson value, $\langle N\rangle$, as in Eq. (2), and consider the contribution of critical fluctuations,

$$\omega_{k,\sigma} = \frac{\kappa_k[N]_\sigma}{\langle N\rangle}, \tag{26}$$

to $\omega_k - 1$ or, more precisely, to $\hat\kappa_k/\langle N\rangle$ (see discussion at the end of Section III B).

This quantity depends on acceptance window and, as expected from the arguments in Section II, saturates in the limit of full (infinite in rapidity y and transverse momentum p_T) acceptance at a value we denote $\omega_{k,\sigma}(\infty)$. To show the acceptance dependence we plot the ratio of $\omega_{k,\sigma}$ in the given acceptance window (Δy in rapidity

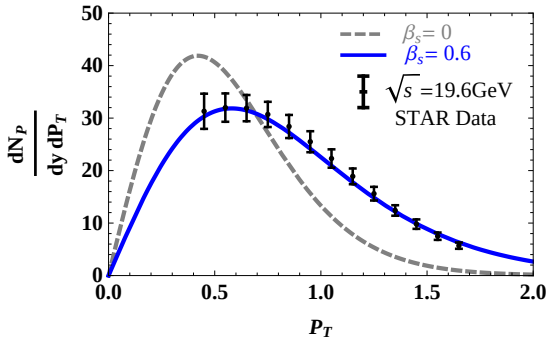

FIG. 3. Spectrum of proton transverse momenta from experiment (points) [52], static thermal distribution (dashed line) and blast-wave model (solid line). p_T is measured in GeV.

for three representative sets of p_T cuts) to the full acceptance value $\omega_{k,\sigma}(\Delta y)/\omega_{k,\sigma}(\infty)$ in Fig. 4. In this ratio the prefactors such as g, ξ and $\tilde{\lambda}_i$ in Eqs. (17)–(19) cancel.

To understand the origin of the Δy scale at which the dependence saturates, it is helpful to look at the thermal rapidity distribution of protons shown in Fig. 2. The width of this distribution essentially sets the scale of the rapidity smearing of correlations (schematically pictured in Fig. 1), and the corresponding $\Delta y_{\rm corr} \sim 1$.

For small $\Delta y \ll 1$, the expected behavior $\omega_{k,\sigma}(\Delta y) \sim (\Delta y)^{k-1}$ comes, in the model, from the factor $(\int_{\hat{A}} \chi_A/\gamma_A)^k \sim (\Delta y)^k$ in Eqs. (17)–(19) where the volume of the integration domain scales as Δy (see Eq. (23)), and from division by $\langle N\rangle \sim \Delta y$ in Eq. (26).

Fig. 4 also demonstrates that the p_T window dependence is significant, especially, for higher-order cumulants. This is a simple consequence of the non-locality of the particle correlations in *momentum* space as seen in, e.g., Eq. (14). In other words, particles of all momenta in the thermal distribution are correlated with each other by critical fluctuations.

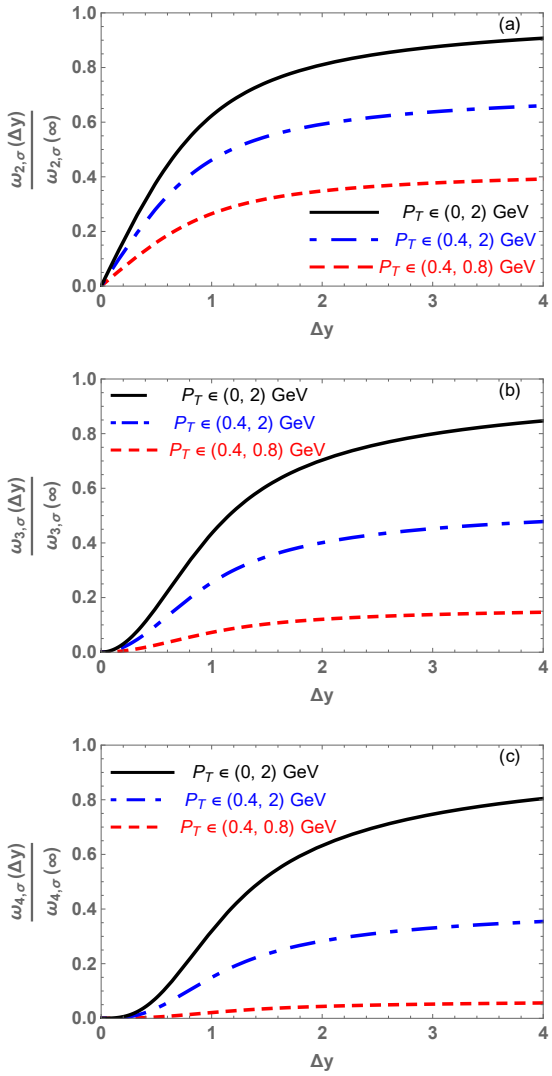

FIG. 4. Acceptance dependence of the critical contribution to the normalized cumulants of proton number. See Section IV.

V. SUMMARY AND CONCLUSIONS

We have described the basic features of the acceptance dependence of the fluctuation measures, in particular, of the (factorial) cumulants of the proton number fluctuations. The main lesson from our analysis is that the dependence on rapidity acceptance window Δy is determined by the correlation range $\Delta y_{\rm corr}$ in momentum space which has very little to do with the correlation length in Bjorken coordinate rapidity η. The latter is related to the spatial correlation length ξ: $\Delta\eta_{\rm corr} \sim \xi/\tau_{\rm f}$ and is typically negligible compared to the former, $\Delta y_{\rm corr} \sim 1$, which is due to the thermal distribution of the particles in the kinematic rapidity. The value $\Delta y_{\rm corr}$ separates two regimes of rapidity window dependence.

For $\Delta y \gg \Delta y_{\rm corr}$ the cumulants grow linearly with Δy and their ratios, such as, e.g, $\kappa_k[N]/\langle N\rangle = \omega_k$, approach constant values.

The opposite, small acceptance regime, $\Delta y \ll \Delta y_{\rm corr}$, is easier to describe using the *factorial* cumulants, $\hat{\kappa}_k$, because they scale as $(\Delta y)^k$ in this regime. The normal cumulants, on the other hand, given by linear combinations of factorial cumulants in Eq. (3), have a more complicated, polynomial dependence on Δy in this regime.

Because the factorial cumulants have much simpler scaling in both large and small acceptance regimes (Eqs. (4), (5)), we conclude that using these cumulants to analyze the acceptance dependence is advantageous.

For the typical experimental acceptance, $\Delta y \lesssim 1$, we find that larger acceptance leads to significantly larger critical point signal, especially for higher-order cumulants of fluctuations (see Fig. 4). Larger p_T acceptance has a

similar effect.[4] These results underscore the importance of the planned STAR detector iTPC upgrade [34] to extend the rapidity coverage for the critical point search in the Beam-Energy Scan experiment at RHIC.

ACKNOWLEDGMENTS

One of the authors (M.S.) would like to thank Berndt Muller, Nu Xu, and ZhangBu Xu for initiating the discussion which lead to this paper, as well as the participants and the organizers of the EMMI Workshop "Fluctuations in Strongly Interacting Hot and Dense Matter: Theory and Experiment" for illuminating discussions. This material is based upon work supported by the U.S. Department of Energy, Office of Science, Office of Nuclear Physics under Award Number DE-FG0201ER41195.

[1] M. A. Stephanov, *Finite Density QCD: Proceedings of the International Workshop, Nara, Japan, July 10-12, 2003*, Prog. Theor. Phys. Suppl. **153**, 139 (2004).
[2] C. Schmidt, *Proceedings, 24th International Symposium on Lattice Field Theory (Lattice 2006)*, PoS **LAT2006**, 021 (2006).
[3] M. A. Stephanov, *Proceedings, 24th International Symposium on Lattice Field Theory (Lattice 2006)*, PoS **LAT2006**, 024 (2006).
[4] S. Gupta, *Proceedings, 5th International Workshop on Critical point and onset of deconfinement (CPOD 2009)*, PoS **CPOD2009**, 025 (2009).
[5] O. Philipsen, *Proceedings, 5th International Workshop on Critical point and onset of deconfinement (CPOD 2009)*, PoS **CPOD2009**, 026 (2009).
[6] C. Schmidt, *Proceedings, 5th International Workshop on Critical point and onset of deconfinement (CPOD 2009)*, PoS **CPOD2009**, 024 (2009).
[7] A. Li, *Proceedings, 27th International Symposium on Lattice field theory (Lattice 2009)*, PoS **LAT2009**, 011 (2009).
[8] K. Fukushima and T. Hatsuda, Rept. Prog. Phys. **74**, 014001 (2011).
[9] G. Aarts, *Proceedings, 30th International Symposium on Lattice Field Theory (Lattice 2012)*, PoS **LATTICE2012**, 017 (2012).
[10] M. A. Stephanov, K. Rajagopal, and E. V. Shuryak, Phys. Rev. Lett. **81**, 4816 (1998).
[11] M. A. Stephanov, K. Rajagopal, and E. V. Shuryak, Phys. Rev. **D60**, 114028 (1999).
[12] V. Koch, in *Chapter of the book "Relativistic Heavy Ion Physics", R. Stock (Ed.), Springer, Heidelberg, 2010* (2010) pp. 626–652.
[13] B. Berdnikov and K. Rajagopal, Phys. Rev. **D61**, 105017 (2000).
[14] D. T. Son and M. A. Stephanov, Phys. Rev. **D70**, 056001 (2004).
[15] G. S. F. Stephans, *Strangeness in quark matter. Proceedings, International Conference, SQM 2007, Levoca, Slovakia, June 24-29, 2007*, J. Phys. **G35**, 044050 (2008).
[16] B. Mohanty, *Proceedings, 21st International Conference on Ultra-Relativistic nucleus nucleus collisions (Quark matter 2009)*, Nucl. Phys. **A830**, 899C (2009).
[17] G. Odyniec, *Proceedings, 8th International Workshop on Critical Point and Onset of Deconfinement (CPOD 2013)*, PoS **CPOD2013**, 043 (2013).
[18] T. Anticic *et al.* (NA49), *Proceedings, 5th International Workshop on Critical point and onset of deconfinement (CPOD 2009)*, PoS **CPOD2009**, 029 (2009).
[19] K. Grebieszkow (NA61/SHINE), *7th International Workshop on Critical Point and Onset of Deconfinement (CPOD 2011) Wuhan, China, November 7-11, 2011*, Central Eur. J. Phys. **10**, 1333 (2012).
[20] S. Ejiri, F. Karsch, and K. Redlich, Phys. Lett. **B633**, 275 (2006).
[21] F. Karsch and K. Redlich, Phys. Lett. **B695**, 136 (2011).
[22] M. A. Stephanov, Phys. Rev. Lett. **102**, 032301 (2009).
[23] M. A. Stephanov, Phys. Rev. **D65**, 096008 (2002).
[24] C. Pruneau, S. Gavin, and S. Voloshin, Phys. Rev. **C66**, 044904 (2002).
[25] A. Bzdak and V. Koch, Phys. Rev. **C86**, 044904 (2012).
[26] M. Sakaida, M. Asakawa, and M. Kitazawa, Phys. Rev. **C90**, 064911 (2014).
[27] M. Kitazawa, *Proceedings, 24th International Conference on Ultra-Relativistic Nucleus-Nucleus Collisions (Quark Matter 2014)*, Nucl. Phys. **A931**, 92 (2014).
[28] M. Kitazawa, Nucl. Phys. **A942**, 65 (2015).
[29] M. Asakawa and M. Kitazawa, (2015), arXiv:1512.05038 [nucl-th].
[30] P. Garg, D. K. Mishra, P. K. Netrakanti, B. Mohanty, A. K. Mohanty, B. K. Singh, and N. Xu, Phys. Lett. **B726**, 691 (2013).
[31] F. Karsch, K. Morita, and K. Redlich, (2015), arXiv:1508.02614 [hep-ph].
[32] S. Jeon and V. Koch, (2003), arXiv:hep-ph/0304012 [hep-ph].
[33] X. Luo (STAR), *Proceedings, 9th International Workshop on Critical Point and Onset of Deconfinement (CPOD 2014)*, PoS **CPOD2014**, 019 (2015).
[34] STAR, *A Proposal for STAR Inner TPC Sector Upgrade (iTPC)* (2015).
[35] J. Bjorken, Phys.Rev. **D27**, 140 (1983).
[36] M. J. Tannenbaum, Phys. Lett. **B347**, 431 (1995).
[37] M. A. Stephanov, Phys. Rev. Lett. **107**, 052301 (2011).
[38] C. Athanasiou, K. Rajagopal, and M. Stephanov, Phys. Rev. **D82**, 074008 (2010).

[4] It is important to also note that the statistical error of the estimator of the cumulants grows *slower* with acceptance in this regime: as $\langle N\rangle^{k/2}$, or $(\Delta y)^{k/2}$. This result is implicit in the analysis of Ref.[53], where the error is estimated by $(\kappa_2/\epsilon)^{k/2}\mathcal{N}_{\rm ev}^{-1/2}$, with $\mathcal{N}_{\rm ev}$ – the number of events and ϵ – the detector efficiency, since, in practice, $\kappa_2 \approx \langle N\rangle$.

[39] J. I. Kapusta, B. Muller, and M. Stephanov, Phys. Rev. **C85**, 054906 (2012).
[40] B. Ling, T. Springer, and M. Stephanov, Phys. Rev. **C89**, 064901 (2014).
[41] E. Schnedermann, J. Sollfrank, and U. W. Heinz, Phys. Rev. **C48**, 2462 (1993).
[42] F. Retiere and M. A. Lisa, Phys. Rev. **C70**, 044907 (2004).
[43] S. A. Voloshin, Phys. Lett. **B632**, 490 (2005).
[44] S. Gavin, L. McLerran, and G. Moschelli, Phys. Rev. **C79**, 051902 (2009).
[45] G. Moschelli and S. Gavin, Nucl. Phys. **A836**, 43 (2010).
[46] L. Jiang, P. Li, and H. Song, (2015), arXiv:1512.06164 [nucl-th].
[47] M. A. Stephanov, Phys. Rev. **D81**, 054012 (2010).
[48] S. Mukherjee, R. Venugopalan, and Y. Yin, Phys. Rev. **C92**, 034912 (2015).
[49] M. Nahrgang, *Proceedings, 9th International Workshop on Critical Point and Onset of Deconfinement (CPOD 2014)*, PoS **CPOD2014**, 032 (2015).
[50] M. Asakawa, S. Ejiri, and M. Kitazawa, Phys. Rev. Lett. **103**, 262301 (2009).
[51] J. Cleymans, H. Oeschler, K. Redlich, and S. Wheaton, Phys. Rev. **C73**, 034905 (2006).
[52] L. Kumar (STAR), *Proceedings, 24th International Conference on Ultra-Relativistic Nucleus-Nucleus Collisions (Quark Matter 2014)*, Nucl. Phys. **A931**, 1114 (2014).
[53] X. Luo, Phys. Rev. **C91**, 034907 (2015).

Appendix A: Small acceptance and factorial cumulants

For completeness, we provide a derivation of the claim, used in Section II, that the k-th factorial cumulant, $\hat{\kappa}_k$, measures the strength of the (connected) k-particle correlation and, therefore, in the regime $\Delta y \ll \Delta y_{\rm corr}$, roughly counts the number of correlated k-plets, leading to $\hat{\kappa}_k \sim (\Delta y)^k$. We shall start with a 2-point correlator and build up to derive Eq. (3) up to $k = 4$ in order to elucidate the relationship between normal and factorial cumulants.

Let us choose an infinitesimally small parameter ε and divide a given kinematic region into $\mathcal{O}(1/\varepsilon)$ infinitesimally small cells, or bins, labeled by index a. We shall denote by n_a the random, fluctuating event-by-event, occupation number of bin a, and by $\langle n_a\rangle$ its event average. When $\varepsilon \to 0$ the value of $\langle n_a\rangle = \mathcal{O}(\varepsilon) \ll 1$ and thus n_a obeys Poisson statistics with infinitesimally small mean. In other words, the probabilities are given by

$$P_{n_a=0} = 1 - \langle n_a\rangle + \mathcal{O}(\varepsilon^2),$$
$$P_{n_a=1} = \langle n_a\rangle + \mathcal{O}(\varepsilon^2),\ P_{n_a\geq 2} = \mathcal{O}(\varepsilon^2). \quad \text{(A1)}$$

i.e., most of the time $n_a = 0$, very seldom $= 1$, and almost never ≥ 2. This means, in particular, that in expectation values we can replace n_a^2 with n_a: $\langle n_a^2 \ldots\rangle = \langle n_a \ldots\rangle \times \big(1 + \mathcal{O}(\varepsilon^2)\big)$. Similarly, we can also derive the following equation for the fluctuation $\delta n_a = n_a - \langle n_a\rangle$ which we shall find useful:

$$\langle (\delta n_a)^k \ldots\rangle = \langle n_a \ldots\rangle \times \big(1 + \mathcal{O}(\varepsilon^2)\big)\,, \qquad (k \geq 2) \quad \text{(A2)}$$

Using this equation we can obtain the following expression for the 2-point correlator:

$$\langle \delta n_a \delta n_b\rangle = \langle n_a\rangle \delta_{ab} + C_{ab} \quad \text{(A3)}$$

The first term on the r.h.s., nonzero only when $a = b$, is simply the contribution of the fluctuation of the number of particles in a given bin a. It does not represent correlations. All correlations are in the second term, C_{ab}, which is nonzero when $a \neq b$. The feature of this term important for us is that in the limit $\varepsilon \to 0$, C_{ab} varies very little within the acceptance window if $\Delta y \ll \Delta y_{\rm corr}$, by definition of $\Delta y_{\rm corr}$.

Let us sum in Eq. (A3) over all the bins within the acceptance window. By definition, $\sum_a n_a = N$, and thus

$$\kappa_2 \equiv \langle (\delta N)^2\rangle = \sum_a \langle n_a\rangle + \sum_{ab} C_{ab} = \langle N\rangle + \hat{\kappa}_2 \quad \text{(A4)}$$

The first term on the r.h.s. is the well-known result of Poisson statistics. The last term is the contribution of correlations. When the acceptance window is much smaller than the range of the correlations, $\Delta y \ll \Delta y_{\rm corr}$, this term is proportional to the volume of the acceptance window squared, $(\Delta y)^2$ or $\langle N\rangle^2$, because in this case we can approximate C_{ab} by a constant within the acceptance window.[5]

Let us generalize this argument to the 3-particle correlator:

$$\langle \delta n_a \delta n_b \delta n_c\rangle = \langle n_a\rangle \delta_{ab}\delta_{ac} + (\delta_{ab} C_{ac} + \delta_{ac} C_{ab} + \delta_{ab} C_{ac}) + C_{abc} \quad \text{(A5)}$$

The 5 terms on the r.h.s. can be represented by diagrams as shown in Fig. 5, where a dot represents a bin and a line connecting two dots represents two bins which coincide, due to, e.g., δ_{ab}. The first term is nonzero only when $a = b = c$ and then it equals $\langle (\delta n_a)^3\rangle = \langle n_a\rangle$ due to Eq. (A2). The next 3 terms (in the parentheses) are nonzero only when 2 of the 3 bins coincide. For example, when $a = b \neq c$, they give $\langle (\delta n_a)^2 \delta n_c\rangle = \langle \delta n_a \delta n_c\rangle = C_{ac}$.

FIG. 5. Diagrammatic representation of the r.h.s. of Eq. (A5)

[5] Note that $C_{ab} = \mathcal{O}(\varepsilon^2)$, but it cannot be neglected compared to the first, $\mathcal{O}(\varepsilon)$, term in Eq. (A3) because in Eq. (A4) the number of elements in the sum $\sum_a$ is $\mathcal{O}(1/\varepsilon)$, while in $\sum_{ab}$ it is $\mathcal{O}(1/\varepsilon^2)$, so the two terms in Eq. (A4) are of the same order, $\mathcal{O}(\varepsilon^0)$, finite in the limit $\varepsilon \to 0$. On the other hand, the diagonal terms, C_{aa}, in Eq. (A3) are negligible, since their contribution to Eq. (A4) is $\mathcal{O}(\varepsilon) \to 0$.

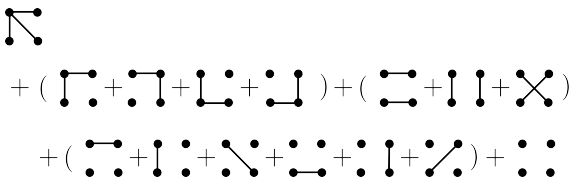

FIG. 6. Diagrammatic representation of the r.h.s. of Eq. (A8)

Summing over the bins within the acceptance we find

$$\kappa_3 \equiv \langle (\delta N)^3 \rangle = \sum_a \langle n_a \rangle + 3 \sum_{ab} C_{ab} + \sum_{abc} C_{abc} = \langle N \rangle + 3\hat{\kappa}_2 + \hat{\kappa}_3 \quad \text{(A6)}$$

It is easy to see that in the regime when the size of the acceptance is much larger than the range of correlations, $\Delta y \gg \Delta y_{\rm corr}$ each term in the r.h.s. scales with the volume of the acceptance window, Δy, or $\langle N \rangle$. While in the opposite regime, small acceptance window $\Delta y \ll \Delta y_{\rm corr}$, due to the smoothness of C_{abc}, the term $\hat{\kappa}_3$ scales as volume to the power 3, or $(\Delta y)^3$.

Defining connected 4-point correlator as usual:

$$\langle \delta n_a \delta n_b \delta n_c \delta n_d \rangle_c \equiv \langle \delta n_a \delta n_b \delta n_c \delta n_d \rangle - (\langle \delta n_a \delta n_b \rangle \langle \delta n_c \delta n_d \rangle + b \leftrightarrow c + b \leftrightarrow d) \quad \text{(A7)}$$

we can express it as

$$\langle \delta n_a \delta n_b \delta n_c \delta n_d \rangle_c = \langle n_a \rangle \delta_{ab}\delta_{ac}\delta_{ad} + (\delta_{ab}\delta_{ac}C_{ad} + \text{ 3 more}) + (\delta_{ab}\delta_{cd}C_{ac} + \text{ 2 more}) + (\delta_{ab}C_{acd} + 5 \text{ more terms}) + C_{abcd} \quad \text{(A8)}$$

We have written only one of the similar terms in each set of the parentheses. The additional terms are easier to represent diagrammatically, as shown in Fig. 6.

Summing over all bins we obtain

$$\kappa_4 \equiv \langle (\delta N)^4 \rangle_c = \langle (\delta N)^4 \rangle - (\langle (\delta N)^2 \rangle)^2 = \sum_a \langle n_a \rangle + 7 \sum_{ab} C_{ab} + 6 \sum_{abc} C_{abc} + \sum_{abcd} C_{abcd} = \langle N \rangle + 7\hat{\kappa}_2 + 6\hat{\kappa}_3 + \hat{\kappa}_4 \quad \text{(A9)}$$

The quantities we denoted by $\hat{\kappa}_k$, and defined so far as k-fold sums of corresponding C's, can be recognized as factorial cumulants of the random variable N (with $\hat{\kappa}_1 = \kappa_1 = \langle N \rangle$). In the same way that normal cumulants (for $k > 2$) measure the deviations from the normal distribution, the factorial cumulants (for $k > 1$) measure deviations from the Poisson distribution.

We find that the scaling of the factorial cumulants with the acceptance window volume, or with Δy, when this window is very small, $\Delta y \ll \Delta y_{\rm corr}$, is given by Eq. (5), while for $\Delta y \gg \Delta y_{\rm corr}$ the scaling is the same as for the normal cumulants, linear in Δy, Eq. (4).

In experiment, the factorial cumulants can be easily calculated from the measured cumulants by solving Eqs. (A4), (A6) and (A9) for $\hat{\kappa}_k$:

$$\hat{\kappa}_1 = \kappa_1 = \langle N \rangle, \quad \hat{\kappa}_2 = \kappa_2 - \kappa_1, \quad \hat{\kappa}_3 = \kappa_3 - 3\kappa_2 + 2\kappa_1, \quad \hat{\kappa}_4 = \kappa_4 - 6\kappa_3 + 11\kappa_2 - 6\kappa_1 \quad \text{(A10)}$$

(the coefficients here are Stirling numbers of the first kind).

Alternatively, one can use the expansion of the generating function:

$$g(x) \equiv \sum_{k=1}^{\infty} \hat{\kappa}_k \frac{x^k}{k!} = \ln \left\langle (1+x)^N \right\rangle . \quad \text{(A11)}$$

to express the factorial cumulants directly in terms of the plain moments $\langle N^k \rangle$, or in terms of the factorial moments $\hat{\mu}_k = \langle N(N-1)\dots(N-k+1) \rangle$ using

$$g(x) = \ln \left(1 + \sum_{k=1}^{\infty} \hat{\mu}_k \frac{x^k}{k!} \right) . \quad \text{(A12)}$$